A Model of Grid Cells Based on a Path Integration Mechanism

Alexis Guanella[1,*] and Paul F.M.J. Verschure[1,2]

[1] Institute of Neuroinformatics, University and ETH Zürich,
CH-8057 Zürich, Switzerland
`guanella@ini.phys.ethz.ch`
[2] ICREA and Technology Department, University Pompeu Fabra
E-08002 Barcelona, Spain

Abstract. The grid cells of the dorsocaudal medial entorhinal cortex (dMEC) in rats show higher firing rates when the position of the animal correlates with the vertices of regular triangular tessellations covering the environment. Strong evidence indicates that these neurons are part of a path integration system. This raises the question, how such a system could be implemented in the brain. Here, we present a cyclically connected artificial neural network based on a path integration mechanism, implementing grid cells on a simulated mobile agent. Our results show that the synaptic connectivity of the network, which can be represented by a twisted torus, allows the generation of regular triangular grids across the environment. These tessellations share same spacing and orientation, as neighboring grid cells in the dMEC. A simple gain and bias mechanism allows to control the spacing and the orientation of the grids, which suggests that these different characteristics can be generated by a unique algorithm in the brain.

Keywords: grid cells, entorhinal cortex, path integration, twisted torus.

1 Introduction

Found in the dorsocaudal medial entorhinal cortex (dMEC) of rats, grid cells [1,2] show increased firing frequency when the animal visits regularly distributed regions in an environment. It has been shown, using auto-correlative maps, that these regions (so-called subfields) form regular triangular tessellations, or grids [1]. It is possible to describe these tessellations, and, thus, the characteristics of a grid cell, with only a few parameters: the orientation and the phase of the grid, and the spacing (minimal inter-subfields distance, i.e. d in this study) and the size of its subfields. Using these parameters, it was shown that grid cells are topographically organized in the dMEC: first, neighboring cells share common orientation and spacing. Second, the spacing of the grid increases isometrically along the dorsoventral axis (in [1], d varies between 39 to 73 cm). Third, the similitude of neighboring grid cells of different layers of the entorhinal cortex, sharing common orientations and spacing, suggests that they are organized in cortical columns [3].

---

[*] Corresponding author.

In spite of these observations, the role of grid cells is still poorly understood. Briefly, it has been proposed that grid cells may be part of a generalized path integration system [1,4], and could be the basis of a metric of spatial relationships [5]. Many arguments verify this hypothesis. First, the grid cell activity and its regular patterns persist after the deprivation of external landmarks (e.g. in the dark [1]). Second, entorhinal lesions disrupt the return path of rats [6]. Third and fourth, suggesting also hard wired mechanisms, the grid structure is expressed instantaneously in novel environments and the spacing parameter seems to be universal (the grid spacing remains constant when increasing the size of the arena) [1]. Fifth, the periodicity of the grid implies a covering of arbitrary big environments. These arguments raise thus the question, how grid cells could be incorporated into a path integration system.

The goal of this article is to describe an artificial neural network implementing grid cells based on a path integration mechanism. In our model, the activity of rate coded neurons is shifted by asymmetric synaptic connections. These connections are modulated by the velocity of the animal, represented by a simulated mobile agent exploring randomly a square arena. The neurons of the network represent a population of neighboring grid cells of the dMEC, whose grids share thus same orientation and spacing, but have different phases. A simple gain and bias mechanism allows the control of the spacing and the orientation of the grid (suggesting that exactly the same algorithm may be used to generate grid cells along the dorsoventral locations of the dMEC). The synaptic connectivity of the network is organized cyclically, and can be represented by a twisted torus. This topology is shown to exactly generate the same regular triangular tessellations of space as grid cells. Stability and robust activity is ensured by attractor dynamics and normalization mechanisms.

2   Methods

2.1   Neurons

We construct a population of N neurons organized in a matrix covering the repetitive rectangular structure of the subfields of grid cells (Fig. 1a). In order to conserve the ratio between the height and the side of an equilateral triangle (which is the core element of a regular triangular tessellation) and in order to have the same density of cells along both x- and y-axes, the number of cells in each row is approximately $2/\sqrt{3}$ times bigger than the number of cells in each column (Fig. 1b).

Activity and Stabilization. The neurons of the network are initialized with a random activity uniformly distributed between 0 and $1/\sqrt{N}$. The activity of a cell i at time $t + 1$, i.e. $A_i(t + 1)$ is defined using a linear transfer function $B_i(t + 1)$ given by

$$B_i(t + 1) = A_i(t) + \sum_{j=1}^{N} A_j(t)\, w_{ji} \ , \tag{1}$$

a   **b**
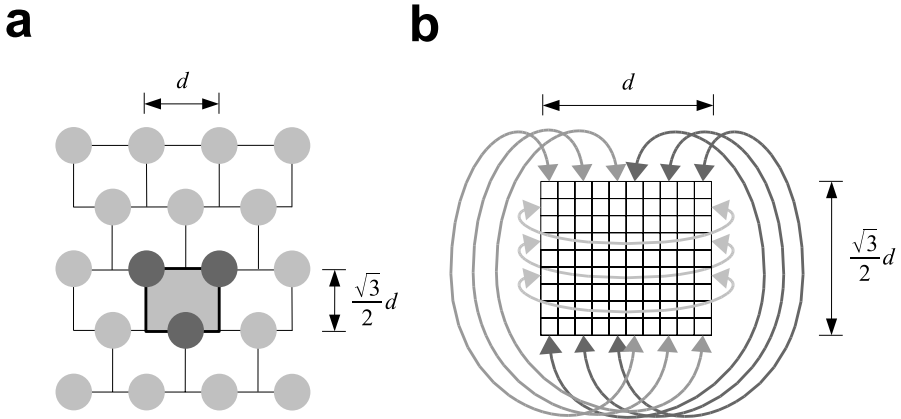
Fig. 1. (a) Repetitive rectangular structure (gray filled rectangle) of the subfields (gray circles) of grid cells defining a regular triangular tessellation of space. **(b)** Matrix of a population of 10×9 grid cells. Neighboring relationships between cells on the side of the structure are represented by gray arrows. For instance, neurons at two opposite vertical sides are neighbors.

where N is the number of cells in the network, w_{ji} is the synaptic weight connecting cell j to cell i, with $i, j \in \{1, 2, ..., N\}$. A floating average normalization mechanism over the cells activity ensures the stability of the network. Thus, $A_i(t+1)$ is defined by

$$A_i(t+1) = B_i(t+1) + \tau \left(\frac{B_i(t+1)}{< B_j(t) >_{j=1}^N} - B_i(t+1) \right) \ , \tag{2}$$

where the function $< \ . \ >_{j=1}^N$ is the mean over the cells of the network, and the parameter τ determines the stabilization strength. To implement this mechanism locally, we use an additional cell (cell $N+1$, which is not a grid cell), that computes the sum of all activities of the grid cells. Normalized by N, the activity of this external cell $< B_j(t) >_{j=1}^N$ is transferred back to the cells of the network. In order to prevent negative cell activities, we set $A_i(t+1) = 0$ when $A_i(t+1)$ is smaller than zero.

2.2   Synapses

The synapses of the network can be divided into two distinct populations. The first population is formed by the synapses which are used to compute the mean activity of the network and to stabilize the cells activity. They connect in both directions all the cells of the network and the external cell $N+1$ (Fig. 2a). Their synaptic weights are all constant and set to 1.

The second population is formed by the synapses implementing the attractor dynamics of the network. These synapses connect each cell i to each cell j, with $i, j \in \{1, 2, ..., N\}$. As we will see, their synaptic weights are computed

as a Gaussian function of the distance between cells (exciting neighboring and inhibiting distal cells (Fig. 2b and 2c)). They are furthermore modulated by the input of the network (i.e. the speed of the mobile agent), which allows to shift the activity packet of the grid cells when the mobile agent is moving.
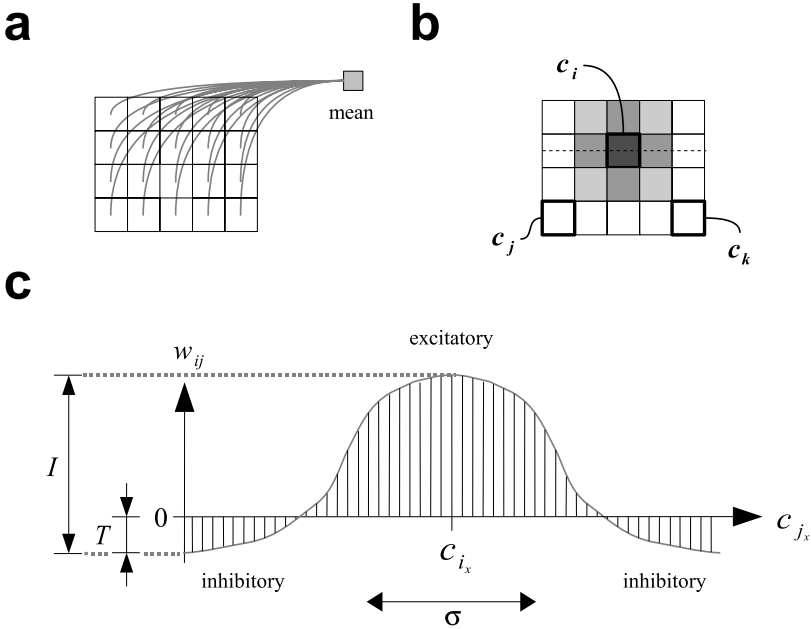
Fig. 2. (a) First population of synaptic weights connecting in both directions all the cells of the network with an external cell used to compute the mean activity. **(b)** Example of synaptic weights of the second population, connecting the neuron c_i to all the cells of the network (including itself). The dark gray color represents a high synaptic weight (e.g. the connection from c_i to itself) and a light gray color a low synaptic weight. The topology of the network implies that c_j and c_k are neighbors. **(c)** Synaptic weights of the cell c_i along an horizontal axis (represented by the dashed line in (b)). Their intensity, shift and width are parametrized respectively by I, T and σ, defining excitatory and inhibitory connections.

Attractor Dynamics. The synaptic patterns connecting grid cells in the network are defined by a Gaussian weight function. We have

$$w_{ij} = I \exp\left(-\frac{||\, c_i - c_j \,||_{tri}^2}{\sigma^2}\right) - T \ , \tag{3}$$

where $c_i = (c_{i_x}, c_{i_y})$ is the position of the cell i, defined respectively by $c_{i_x} = (i_x - 0.5)/N_x$ and by $c_{i_y} = \frac{\sqrt{3}}{2}(i_y - 0.5)/N_y$ (with $i_x \in \{1, 2, ..., N_x\}$ and $i_y \in \{1, 2, ..., N_y\}$), and where N_x and N_y are the number of columns and rows in the cells matrix (Fig. 1) and i_x and i_y the column and the row numbers of cell i. I is the intensity parameter, defining the overall strength of the synapses,

σ regulates the size of the Gaussian and T is the shift parameter determining excitatory and inhibitory zones (Fig. 2c). The norm $||\,.\,||_{tri}$ defines the induced metric $\text{dist}_{tri}(.,.)$ of the network. To obtain the repetitive rectangular structure of the grid subfields, the cells at the border of the layer have to be neighbors of the cells at the opposite border (as an example, the two grid cells j and k on Fig. 2a should be neighbors). This can be seen as a torus topology. However, this is not sufficient to form a triangular grid, since a simple torus would lead, in our model, to a rectangular tessellation of space. The regular triangular tessellation is generated by twisting the torus. This is represented in the definition of the distance $\text{dist}_{tri}(.,.)$ or the norm $||\,.\,||_{tri}$ which permits to obtain regular triangular tessellations:

$$\text{dist}_{tri}(\boldsymbol{c_i}, \boldsymbol{c_j}) := ||\,\boldsymbol{c_1} - \boldsymbol{c_2}\,||_{tri} = \min_{j=1}^{7} ||\,\boldsymbol{c_1} - \boldsymbol{c_2} + \boldsymbol{s_j}\,||\ , \tag{4}$$

where

$$\boldsymbol{s_1} := (0,0)\ , \tag{5}$$

$$\boldsymbol{s_2} := (-.5, \frac{\sqrt{3}}{2})\ , \tag{6}$$

$$\boldsymbol{s_3} := (-.5, -\frac{\sqrt{3}}{2})\ , \tag{7}$$

$$\boldsymbol{s_4} := (.5, \frac{\sqrt{3}}{2})\ , \tag{8}$$

$$\boldsymbol{s_5} := (.5, -\frac{\sqrt{3}}{2})\ , \tag{9}$$

$$\boldsymbol{s_6} := (-1, 0)\ , \tag{10}$$

$$\boldsymbol{s_7} := (1, 0)\ , \tag{11}$$

and where $||\,.\,||$ is the Euclidean norm.

Modulation. The input of the network is the speed vector $\boldsymbol{v} := (v_x, v_y)$, which represents the speed of the mobile agent. This input doesn't depend on any absolute information about location. The maximum velocity of the mobile agent is given by the parameter v_{max} such as $||\,v\,||$ is always smaller than v_{max}.

It is possible to increase or decrease the size and the spacing of the subfields, as well as changing the orientation of the grid by changing only two parameters in the model, i.e. the gain $\alpha \in \mathbb{R}^+$ and bias $\beta \in [0, \pi/3]$. The input of the network is thus modulated and biased by the gain and the bias parameters, with

$$\boldsymbol{v} \longmapsto \alpha\, \boldsymbol{R_\beta} \boldsymbol{v}\ , \tag{12}$$

where $\boldsymbol{R_\beta}$ is the rotation matrix of angle β defined by

$$\boldsymbol{R_\beta} = \begin{pmatrix} \cos(\beta) & -\sin(\beta) \\ \sin(\beta) & \cos(\beta) \end{pmatrix}\ . \tag{13}$$

The activity pattern is stable when the mobile agent stays immobile. However, when the agent moves, the synaptic connections of the network shift in the

direction of the speed vector of the robot (Fig. 3). When expressing the synaptic weight as a function of time, we have

$$w_{ij}(t+1) = I \exp\left(-\frac{\|\,\boldsymbol{c_i} - \boldsymbol{c_j} + \alpha\,\boldsymbol{R_\beta}\,\boldsymbol{v}(t)\,\|_{tri}^2}{\sigma^2}\right) - T \ . \tag{14}$$

a

b

$\boldsymbol{v}$

modulation

$\boldsymbol{c}_i$

$\boldsymbol{c}_i$
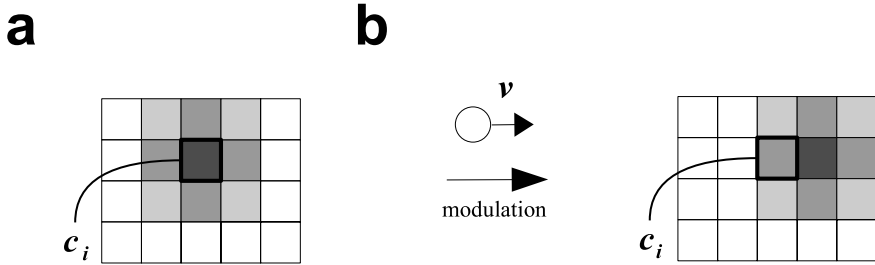
Fig. 3. Modulation of the synaptic connections of cell i. **(a)** Before modulation, the synaptic pattern of the cell i is centered around $\boldsymbol{c_i}$. **(b)** After modulation, the synaptic pattern is shifted proportionally in the direction of the speed $\boldsymbol{v}$ of the mobile agent.

2.3 Mobile Agent and Environment

The experiments are performed using a simulated Khepera robot (K-Team, Yverdon, Switzerland), which randomly explores a square arena. When approaching a wall, a Braitenberg control algorithm [7] is activated to avoid collisions. The size of the square arena is 1×1 meter, such as one arena side is approximately 18 times bigger than a robot diameter (.055 meter).

2.4 Parameters

The values of the parameters used in this study are given in table 1. These values have to satisfy two criteria. First, they have to ensure the stability of the cells of the network. This means for instance that the cells activity should not be growing endlessly. Second, they must induce the attractor dynamics of the network, and

Table 1. Values of the parameters used in this study

Parameter		Value	Unit
N	=	90	[cell]
N_x	=	10	[cell]
N_y	=	9	[cell]
τ	=	0.8	[no unit]
I	=	0.3	[no unit]
σ	=	0.24	[meter]
T	=	0.05	[no unit]
v_{max}	=	0.0275	[meter/time step]

therefore a single and stable activity packet should be continuously observed in the cell population. These criteria have to be tested over a large number of time steps. Since no objective or cost function is given in this study, no parameter search for optimization is computed.

3   Results

To analyze the activity of the neurons of the network, we first computed their mean activity maps, i.e. the mean activity of a cell as a function of the position of the mobile agent (Fig. 4). These maps show the coherent and stable activity of the multiple grid subfields. To determine if these subfields were organized in a regular triangular tessellation, we fitted the mean activity maps to regular triangular tessellations composed of Gaussian subfields. We computed the mean square residuals over all the network cells, and found the value of 0.0028 +/- 0.0004 (mean +/- standard deviation (std.)). The mean square residuals for each cell were always smaller than 0.005. These results strongly suggest that our model generates regular triangular tessellating subfields. Note that in order to get coherent results for this computation, we normalized the mean activity maps such as the maximum and the minimum intensity of these maps were respectively 1 and 0. The stability of the network was assessed by running experiments over an extended number of time steps (repetitively stable when tested over 1 million time steps).

Gain and Bias. An interesting feature of the network is the possibility to vary the spacing and the orientation of the grids by just varying the gain and bias parameters. As shown in Figs. 4 and 5, higher gain values lead to denser grids (and therefore smaller spacing between subfields) whereas higher bias values rotate the grids. We made a regression analysis to model and determined the relationship between the gain and the bias parameters and respectively the spacing and the orientation of the grids. For the gain, we found $y = a + b \log_2(x)$ with $a = -0.90$ and $b = -0.39$, with mean least square residuals of 0.00016, and where x and y are respectively gain and grid spacing. For the bias, we found $y = a + bx$ with $a = 0.00$ and $b = 1.00$, with mean least square residuals of 0.00004, and where x and y are respectively bias and grid orientation.

4   Discussion

In this article, we have presented a model of grid cells based on path a integration mechanism, embedded on a simulated mobile agent. We have shown that the neural activity of the network generates regular triangular tessellations of the environment, as grid cells in the dMEC. In our model, the grids cells share same orientation and spacing, as neighboring grid cells in the dMEC, and, as suggested in [3], as grid cells in cortical columns of the dMEC. A simple gain and bias mechanism on the input allows to vary, respectively in a log-linear and a linear relationship, the spacing and the orientation of the grids. Our model

a

Cell 14/90

Gain 0.05   Gain 0.06   Gain 0.07   Gain 0.08   Gain 0.09

Cell 61/90

Gain 0.05   Gain 0.06   Gain 0.07   Gain 0.08   Gain 0.09

b

Cell 25/90

Bias 0.00 [rad]   Bias 0.22 [rad]   Bias 0.44 [rad]   Bias 0.66 [rad]   Bias 0.88 [rad]

Cell 74/90

Bias 0.00 [rad]   Bias 0.22 [rad]   Bias 0.44 [rad]   Bias 0.66 [rad]   Bias 0.88 [rad]
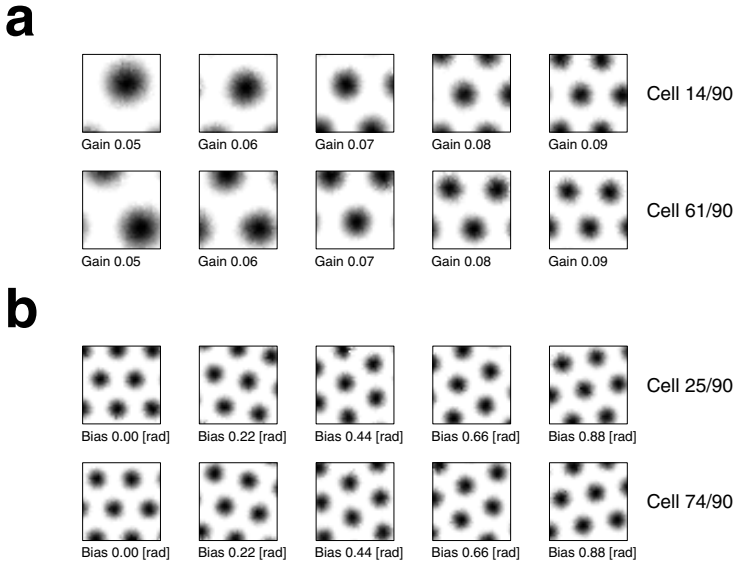
Fig. 4. (a) Mean activity maps of two grid cells with different gain values (here, the bias value is set to zero). Dark regions and light regions represent respectively high and low mean activity. These maps were computed over 50000 time steps. The discretization of the arena correspond to 40×40 bins. **(b)** Mean activity maps of two grid cells with different bias values (here, the gain value is set to 0.11).

gives thus a concrete example of a cortical circuit which can implement in a same algorithm grid cells with different spacings and orientations. In the dMEC, the spacing of the grid isometrically increases along the dorsoventral axis, which could thus suggest an exponential increase of the rat velocity gain along this axis.

Many studies present the implementation of path integration mechanisms based on attractor dynamics [8,9,10,11]. The idea to apply these methods for grid cells was first presented in [1] and described further in [4]. It has been implemented first in [12], as a symmetric locally connected neural network. Here, it is the first time that an implementation of such a system is explicitly described and implemented on a cyclically connected map. This synaptic architecture, which can be represented by a twisted torus, is new, and was shown in this study to be able to generate effectively grid cells with regular triangular tessellating subfields. The advantages of such a system is that it allows to implement in a relatively small population of cells a representation of space covering arbitrary big environments. Moreover, because of this particular synaptic connectivity, all the network cells have regular triangular tessellating subfields.

Our model of grid cells may be used as the proprioceptive element of a robust, modulatory and biologically based navigational system combining idiothetic (internal) and allocentric (external) sensory inputs. On the first hand, one of the classical problem of path integration mechanisms is the accumulation of
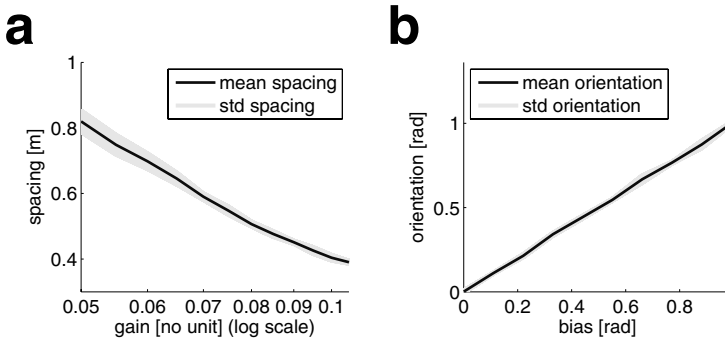
Fig. 5. (a) Spacing of the grid as a function of the gain parameter. **(b)** Orientation of the grid as a function of the bias parameter.

proprioceptive errors over time. For instance, in our model, the mean activity maps of grid cells would collapse if we would introduce noise in the speed input. On the other hand, one of classical problem of allocentric systems is their inability to disambiguate between two similar inputs. For instance, realistic models of place cells [13,14] of the hippocampus, based on visual inputs (e.g. [15]) are not able to distinguish between two visually similar places. A combination of these two approaches would be useful to deal with their respective weaknesses. Allocentric place cells (e.g. based on vision) would be used to recalibrate the activity of the grid cells in case of path integration errors, and, in turn, the activity of grid cells could be used to generate place cells (using simple a simple Hebbian mechanism as proposed in [4]), able to disambiguate between two visually similar places. The location of the dMEC, upstream the hippocampus, which is, in turn, an afferent of the entorhinal cortex, provides an anatomical basis for such a modulatory system.

Acknowledgments

References

1. Hafting, T., Fyhn, M., Molden, S., Moser, M.B., Moser, E.I.: Microstructure of a spatial map in the entorhinal cortex. Nature **436**(7052) (2005) 801–6
2. Fyhn, M., Molden, S., Witter, M.P., Moser, E.I., Moser, M.B.: Spatial representation in the entorhinal cortex. Science **305**(5688) (2004) 1258–64
3. Moser, M., Sargolini, F., Fyhn, M., Hafting, T., Witer, M., Moser, E.: Grid cells in medial entorhinal cortex: indications of columnar organization. Soc Neurosci Abstr **198**(4) (2005)

4. O'Keefe, J., Burgess, N.: Dual phase and rate coding in hippocampal place cells: theoretical significance and relationship to entorhinal grid cells. Hippocampus **15**(7) (2005) 853–66
5. Jeffery, K.J., Burgess, N.: A metric for the cognitive map: found at last? Trends Cogn Sci **10**(1) (2006) 1–3
6. Parron, C., Save, E.: Evidence for entorhinal and parietal cortices involvement in path integration in the rat. Exp Brain Res **159**(3) (2004) 349–59
7. Braitenberg, V.: Vehicles, experiments in synthetic psychology. MIT Press (1984)
8. McNaughton, B., Barnes, C., Gerrard, J., Gothard, K., Jung, M., Knierim, J., Kudrimoti, H., Qin, Y., Skaggs, W., Suster, M., Weaver, K.: Deciphering the hippocampal polyglot: the hippocampus as a path integration system. J Exp Biol **199** (1996) 173–85
9. Samsonovich, A., McNaughton, B.: Path integration and cognitive mapping in a continuous attractor neural network model. J Neurosci **17**(15) (1997) 5900–20
10. Stringer, S., Rolls, E., Trappenberg, T., de Araujo, I.: Self-organizing continuous attractor networks and path integration: two-dimensional models of place cells. Comput Neural Syst **13**(4) (2002) 429–46
11. Conklin, J., Eliasmith, C.: A controlled attractor network model of path integration in the rat. J Comput Neurosci **18**(2) (2005) 183–203
12. Fuhs, M.C., Touretzky, D.S.: A spin glass model of path integration in rat medial entorhinal cortex. J Neurosci **26**(16) (2006) 4266–76
13. O'Keefe, J., Dostrovsky, J.: The hippocampus as a spatial map. Preliminary evidence from unit activity in the freely-moving rat. Brain Res **34**(1) (1971) 171–5
14. O'Keefe, J., Nadel, L.: The hippocampus as a cognitive map. Clarendon Press, Oxford (1978)
15. Wyss, R., König, P., Verschure, P.F.M.J.: A model of the ventral visual system based on temporal stability and local memory. PLoS Biol **4**(5) (2006) e120